Clays and Clay Minerals, Vol. 22, pp. 127–137. Pergamon Press 1974. Printed in Great Britain

INTERNAL AND EXTERNAL MORPHOLOGY OF TUBULAR AND SPHEROIDAL HALLOYSITE PARTICLES*

J. B. DIXON† and T. R. MCKEE‡

Texas A & M University, College Station, Texas 77843, U.S.A.

(*Received* 1 *September* 1973)

Abstract—Tubular halloysite from Wagon Wheel Gap, Colorado and spheroidal halloysite from Redwood County, Minnesota were examined by transmission electron microscopy. Clay samples were prepared by the following techniques: drop-mounted suspension on carbon support films; thin sections of clay in Araldite epoxy resin; and carbon–platinum–palladium single-stage replicas.

Both types of dehydrated halloysite have interlayer separations between packets of layers. Halloysite tubes are composed of packets as thin as five layers which sometimes reveal a rolled interior configuration in cross-sectional view. Thicker tubes are composed of many layers per packet. Some large tubes appear in cross section as folded packets of layers. The interior morphology of spheroidal halloysite particles is more irregular and the layer structure is more discontinuous than in most tubes. The spheroidal halloysite of this study is characterized by external tangential plates with hexagonal shape suggestive of kaolinite.

Halloysite occurs in different morphological forms (Bates, 1971). Tubular and spheroidal halloysite have a wide geographic occurrence in soils and weathered rocks (Askenasy *et al.*, 1973; Parham, 1969). The arrangements of kaolin layers in these different shaped particles are of considerable interest. Chukhrov and Zvyagin (1966) reported polyhedral halloysite tubes made up of radial zones of plates parallel to the tube axis and clearance between radial zones was observed. The objective of this study was to determine the fine morphological properties of two important halloysite types using several electron microscopy techniques.

METHODS AND MATERIALS

Tubular halloysite from Wagon Wheel Gap, Colorado obtained from Ward's Natural Science Establishment, Rochester, New York and spheroidal halloysite from Redwood County, Minnesota (courtesy Dr. W. E. Parham, Minneapolis, Minnesota) were dispersed and fractionated according to Jackson (1956, p. 31). Clays were fractionated in pH 10 Na_2CO_3 solution after carbonates, organic matter and free Fe–oxides had been removed. Samples were prepared for X-ray diffraction analysis by the methods of Jackson. Diffraction analyses were made with a Philips vertical goniometer equipped with a graphite monochromator to provide Cu Kα radiation.

Samples were prepared for study with the electron microscope in three ways. Dilute aqueous suspensions of clay samples were drop-mounted on carbon support films with a micro-pipette and dried in a desiccator. Thin sections were prepared by an Araldite epoxy resin technique similar to that of Brown and Rich (1968). Replicas were prepared of clay suspensions dried on freshly cleaved mica sheets by double shadowing with 80 per cent platinum–20 per cent palladium and subsequently sputtering on a thin layer of carbon. The clay-containing carbon replicas were then floated off the mica onto distilled water and the clay was etched away by several changes of HF solution. Electron micrographs were made with an Hitachi HU11E electron microscope at 100 kV, except where indicated.

RESULTS AND DISCUSSION

X-ray diffraction analysis

The tubular halloysite gave characteristic X-ray peaks at 7·14 and 3·57 Å for a kaolin group mineral (Fig. 1a). Some interlayer hydration of the 0·2–0·08 μm clay was indicated by a slight hump near 11 Å. The tubular sample would not qualify as halloysite by the criterion of Brindley (1961) which requires the 4·45 Å peak to be more than half the intensity of the first order peak. This kaolinite-like behavior may be largely produced by some flattened and polyhedral particles as discussed later. A few hexagonal plates observed with the tubes probably account for a small but unknown part of the intensity of basal reflections. The sharpness of the 7·14 Å peak also is more characteristic of kaolinite than of many halloysites.

* The investigations were supported by the Texas Agricultural Experiment Station, Texas A & M University, College Station, Texas 77843, U.S.A.

† Professor of Soils, Department of Soil and Crop Sciences.

‡ Graduate Assistant, Department of Oceanography.

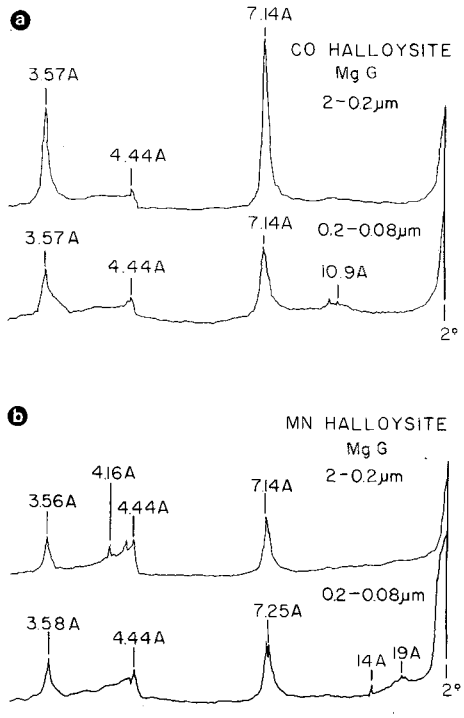

Fig. 1. X-ray diffraction curves for Mg-saturated and glycerol solvated 2–0·2 μm and 0·2–0·8 μm. (a) Tubular halloysite from Colorado (CO); (b) spheroidal halloysite from Minnesota (MN).

X-ray diffraction patterns of spheroidal halloysite are fairly characteristic of a dehydrated halloysite with 4·44 Å peaks at least half the intensity of the (001) peaks (Fig. 1b). Small amounts of impurities are evident in the medium clay; peaks at 14 and 19 Å are suggestive of vermiculite or chlorite and smectite, respectively.

Tubular halloysite morphology

Tubular halloysite from Wagon Wheel Gap is characterized by particles with considerable variation in dimensions ranging from long thin tubes to short thick ones (Fig. 2). The polyhedral morphology of the tubes, particularly the shorter ones, is shown in Figs. 2(a) and in 3(e). The sides of the polyhedra appear more regular in the side view in a replica (Fig. 3e) than in the end view of Fig. 2(a). The irregular polyhedral cross-sections of particles (Figs. 2a and 4e) seem to have been influenced by varied external confining forces rather than uniform forces which would result in regular crystallographic angles. Hexagonal growth edges of tubular halloysite consistently have an edge perpendicular to the direction of the tube axis, Figs. 3(a, b and d) (arrows). The orientation of the layers with respect to the tube axis appears to be crystallographically controlled.

Light interlayer separations are visible in cross sectional and longitudinal views of many tubular particles. Separations occur frequently in small dia. particles (Figs. 2b, d and Fig. 4a). Interlayer separations are largest near corners of small polyhedral particles and near particle centers (Fig. 4e). Interlayer separations parallel to the axis of two wide tubes are visible in longitudinal sections (solid arrows, Fig. 4f). The longitudinal separations divide the particles into packets with thicknesses equivalent to about 35 layers (35 × 7·2 Å = 252 Å). The thick packets and intervening layer separations are repeated up to six times in a given particle.

A relationship between packet thickness and particle diameter is shown in Table 1. Measurements of packets were made from the outside of the particle to an internal light line or region (layer separation) and perpendicular to the plane of the layers. Measurements

Table 1. Packet thickness vs cross-sectional dimensions of tubular halloysite particles

Average packet thickness (Å)	7·2 Å layers per packet	Particle dimension* Maximum (Å)	Minimum (Å)
34	5	260	220
36	5	280	210
38	5	370	340
44	6	520	*ND*
80	11	770	730
103	15	390	270
171	24	870	*ND*
193	27	810	590
262	36	1510	1070
276	38	1230	780

* 0·2–0·08 μm Wagon Wheel Gap, Colorado halloysite.
ND = not determined.

https://doi.org/10.1346/CCMN.1974.0220118 Published online by Cambridge University Press

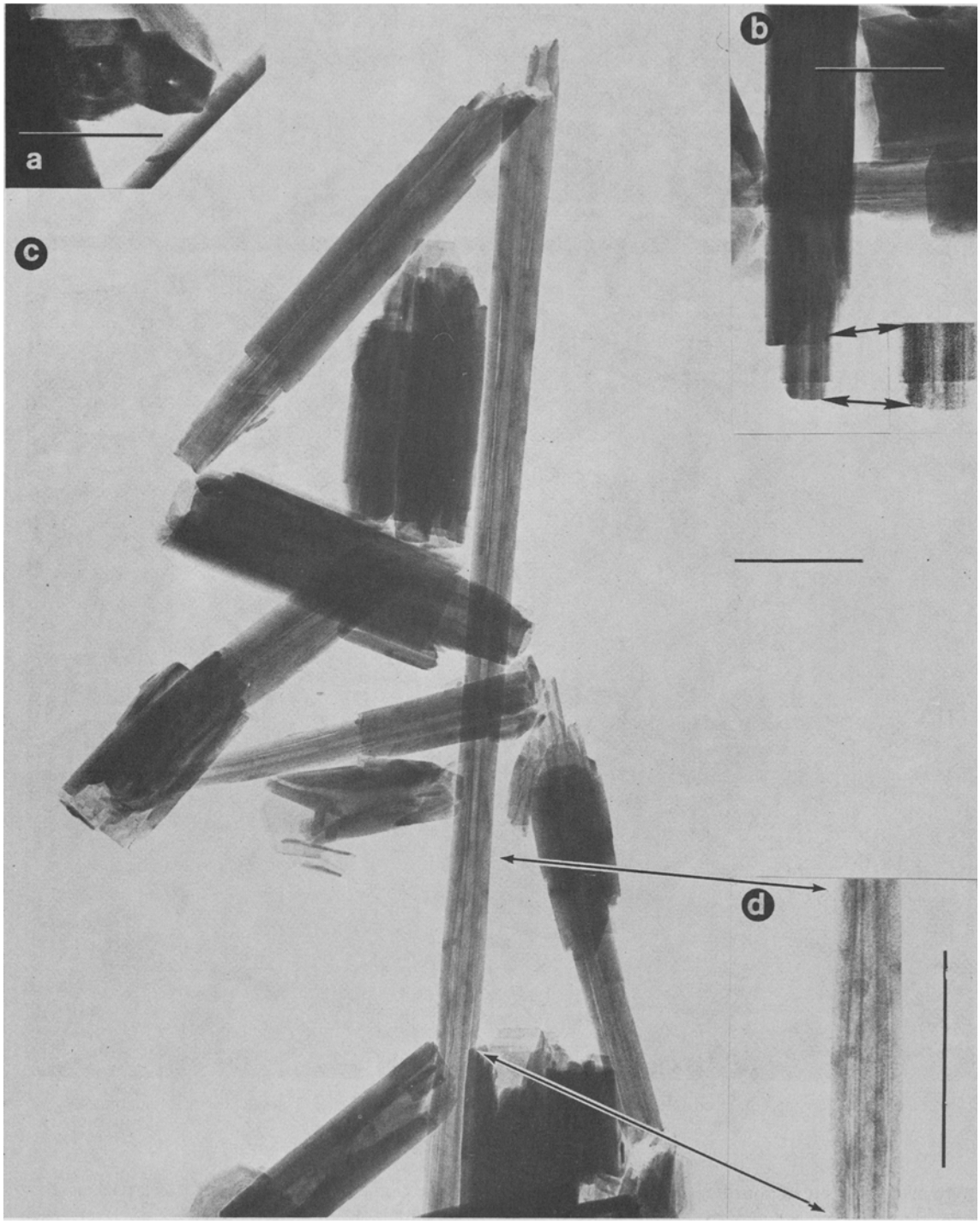

Fig. 2. Transmission electron micrographs of tubular halloysite. Particle size fraction represented is 2–0·2 μm. These micrographs were made at 75 kV. The reference line is 0·2 μm in all micrographs.

https://doi.org/10.1346/CCMN.1974.0220118 Published online by Cambridge University Press

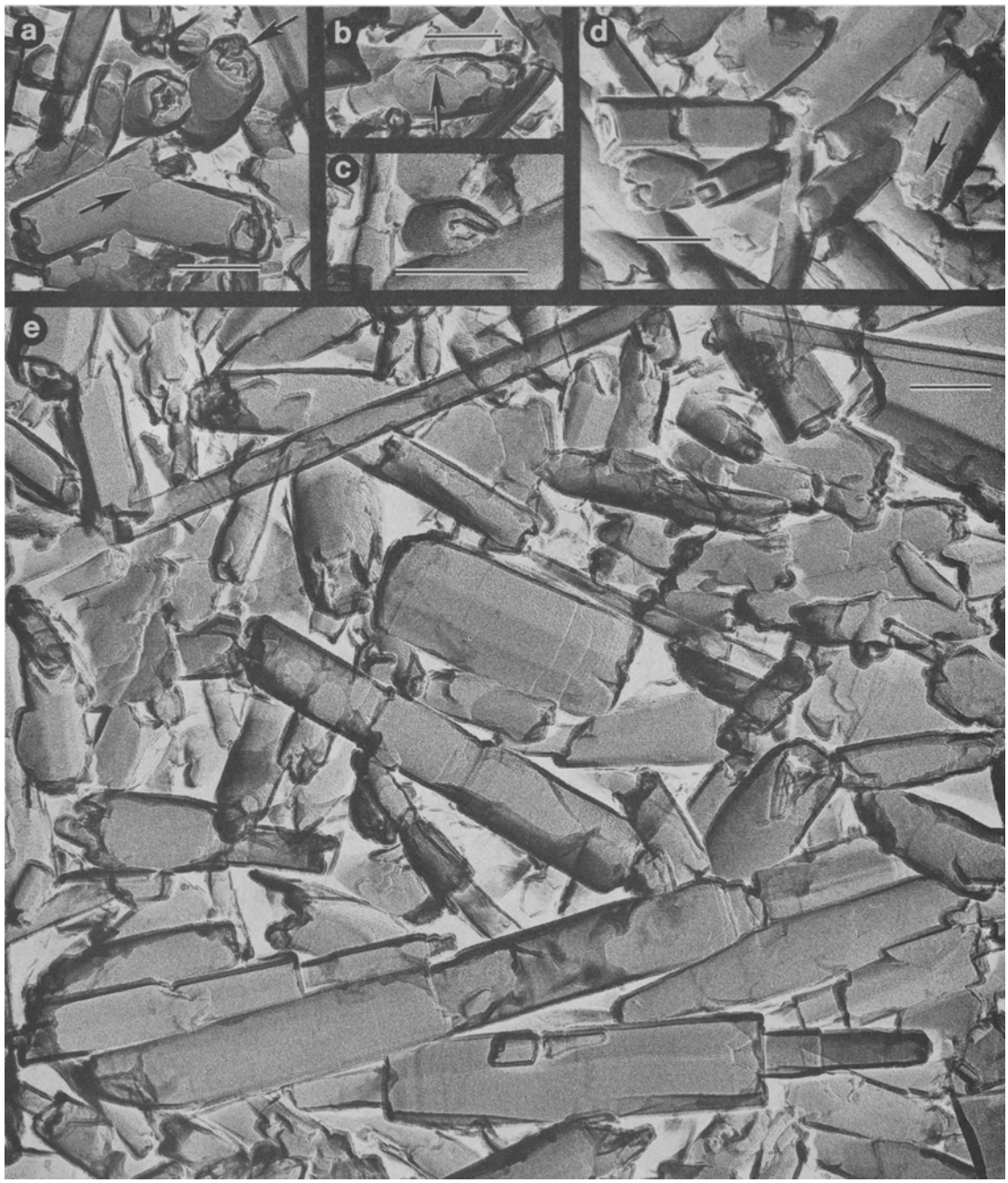

Fig. 3. Transmission electron micrographs of replicas of tubular halloysite. The particle size fraction is 2–0·2 μm except for (c) which is 0·2–0·08 μm.

were made only on sectioned particles. The loose roll of the layer assemblage in particles such as the one in Fig. 4(a) (arrow) permitted averaging packet thickness from measurements taken in several different parts of the particle. Tubes made up of thin packets of about 5 layers each are smaller and more nearly circular in cross-section than particles having thick packets. Particles composed of thick packets 27–38 layers each show flattening in cross-sectional view. The latter type of particle has some similarity to kaolinite in that some parts of the particle are planar. Some particles occur as a simple folded packet of layers (Fig. 4f, F). Growth

Fig. 4. Transmission electron micrographs of thin sections of tubular halloysite 2–0·2 μm clay except (a) and (f) which are 0·2–0·08 μm. The particle in (e) was completely surrounded by mounting resin in the plane of the photograph but the resin may not be evident in the plate.

https://doi.org/10.1346/CCMN.1974.0220118 Published online by Cambridge University Press

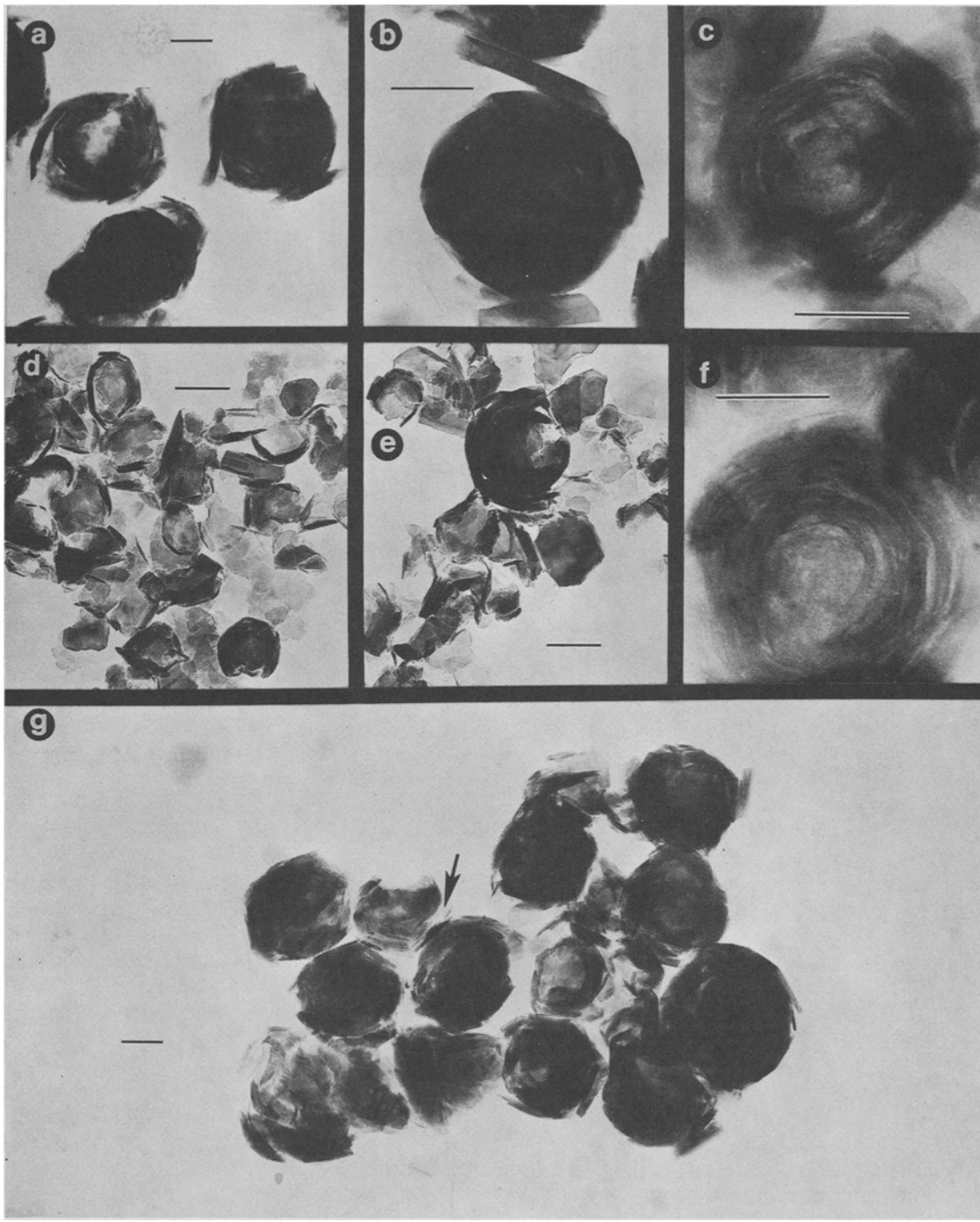

Fig. 5. Transmission electron micrographs of spheroidal halloysite taken at 100 kV (d, e), at 200 kV (a, b, g) and 800 kV (c, f). The samples are water dispersed whole clay except (d) and (e) which are 0·2–0·08 μm clay.

https://doi.org/10.1346/CCMN.1974.0220118 Published online by Cambridge University Press

apparently proceeded somewhat like kaolinite in the thick, folded particles because the layers do not extend beyond one revolution. The planar parts of the halloysite particles would contribute to enhanced basal X-ray diffraction intensities as compared to cylindrical particles.

Evidence for a rolled configuration of layers is shown in Figs. 4(a and d) (arrows) where packets of layers appear to extend out from the rolls. Growth in a roll-like fashion is suggested by Fig. 3(a) (upper arrow) and (b) (arrow). Particles that appear to have a rolled assemblage of layers are suggested at other places in Fig. 4(f) (open arrows). Some particles (e.g. Fig. 4(a), arrow) show several revolutions of a thin-layer packet. Yada (1967) has reported a rolled configuration of layers in chrysotile tubes also viewed along the tube axis of sectioned particles.

Spheroidal halloysite morphology

Viewing the spheroidal halloysite from Minnesota by transmission electron microscopy is restricted by particle thickness and consequent scattering and absorbance of the electron beam. The darkest circular particle in Fig. 5(e) is opaque to the 100 kV electron beam on one side and thins toward the open side revealing some detail of curved layers and material in the interior of the particle. Figures 5(a, b and g) were taken at 200 kV, and Figs. 5(c and f) were taken at 800 kV to improve electron beam penetration. Many interlayer separations are visible in the high voltage pictures whereas little interior detail can be seen in whole spheroids viewed at 100 and 200 kV.

The growth of external particles tangential to the spheres is one of their most prominent features (Figs. 5a, b and g). External platyness is evident in replicas (Fig. 6(g), P's). The external plates have the 120° angles characteristic of kaolinite. Also, the platyness of the layer structure of spheroidal halloysite is evident well into the wall of some particles (e.g. Fig. 5(g) arrow).

Peeling of external spheroidal halloysite layers is particularly evident in Fig. 5(a). Some fragments and plates in Fig. 5(d and e) may have been produced by peeling of spheroids. The broken circular particles of Figs. 5(d and e) have retained interior material indicating the resistance of spheroidal halloysite component parts to dispersion treatments.

Replicas of spheroidal halloysite show a spherical aspect of the particles (Fig. 6). The general view of these whole particles is that of spheroids having a patchy exterior of kaolin plates. Holes and cavities are evident in several particles. Although the interior and exterior of some particles have flat platy sections, as mentioned earlier, the curvature of internal layers is most evident in Fig. 6(c).

Thin sections (Fig. 7) reveal edge views of packets of layers in circular or elliptical patterns. In addition, the core of the spheroids is different from the external layer morphology. If the center is platy, the central layer-orientation (e.g. in Figs. 7b and d) is different from that of the exterior layers. As seen in transmission photos (Fig. 5), and sections (Fig. 7), the core is frequently less dense than the exterior part suggesting a cavity (also shown in Figs. 6d and e). The accommodation of the layer structure to a spheroidal shape appears to have resulted in layer separations between packets of layers along the z-axis and interruptions at intervals in the a–b plane. These interruptions of crystal continuity are particularly evident in transmission pictures (Figs. 5c, f and g) and in sectioned particles. Some disruption may be a product of the sectioning process.

GENERAL DISCUSSION

The Minnesota (MN) spheroidal halloysite has a platy exterior and the plates have the hexagonal shape characteristic of kaolinite. Weathering of halloysite to kaolinite has long been thought to occur based on mineral association, and such a transformation has been proposed by Kittrick (1969) from solubility data. The occurrence of the MN halloysite in a Cretaceous clay (Parham, 1970) indicates that it has had a long time for recrystallization. Halloysite spheroids in a soil on Quaternary volcanic rocks of Guatemala (Askenasy *et al.*, 1973) and those from a very youthful volcanic surface soil of Mexico (Dixon and McKee, in press) did not show the frequent tangential platy particles evident in the halloysite reported here. Some platyness may have developed in surfaces of halloysite "polyhedra" and spheres from Japan but the development of these features is difficult to evaluate from the data available (e.g. Bates, 1971).

The interior of halloysite tubes and spheroids is often more transparent to the electron beam than the exterior, and the core is sometimes hollow. Measurements of the less absorbing cores indicate a dia. of about 1500 Å in the spheres (Figs. 5c and f) and an average of 180 Å for tubes (Figs. 2 and 4). The nine tubes measured had core diameters from 70 to 380 Å. The measurements indicate a markedly smaller core diameter for the tubes than the spheres. The greater curvature of the halloysite layers around the core seems to be a function of the thinner packets of layers in the small halloysite tubes. Also, two-dimensional curvature (tubular) is structurally more favorable than three-dimensional curvature (spheroidal). Greater discontinuity between and along packets in spheroids than in tubes indicates more structural disorder in spheroids.

https://doi.org/10.1346/CCMN.1974.0220118 Published online by Cambridge University Press

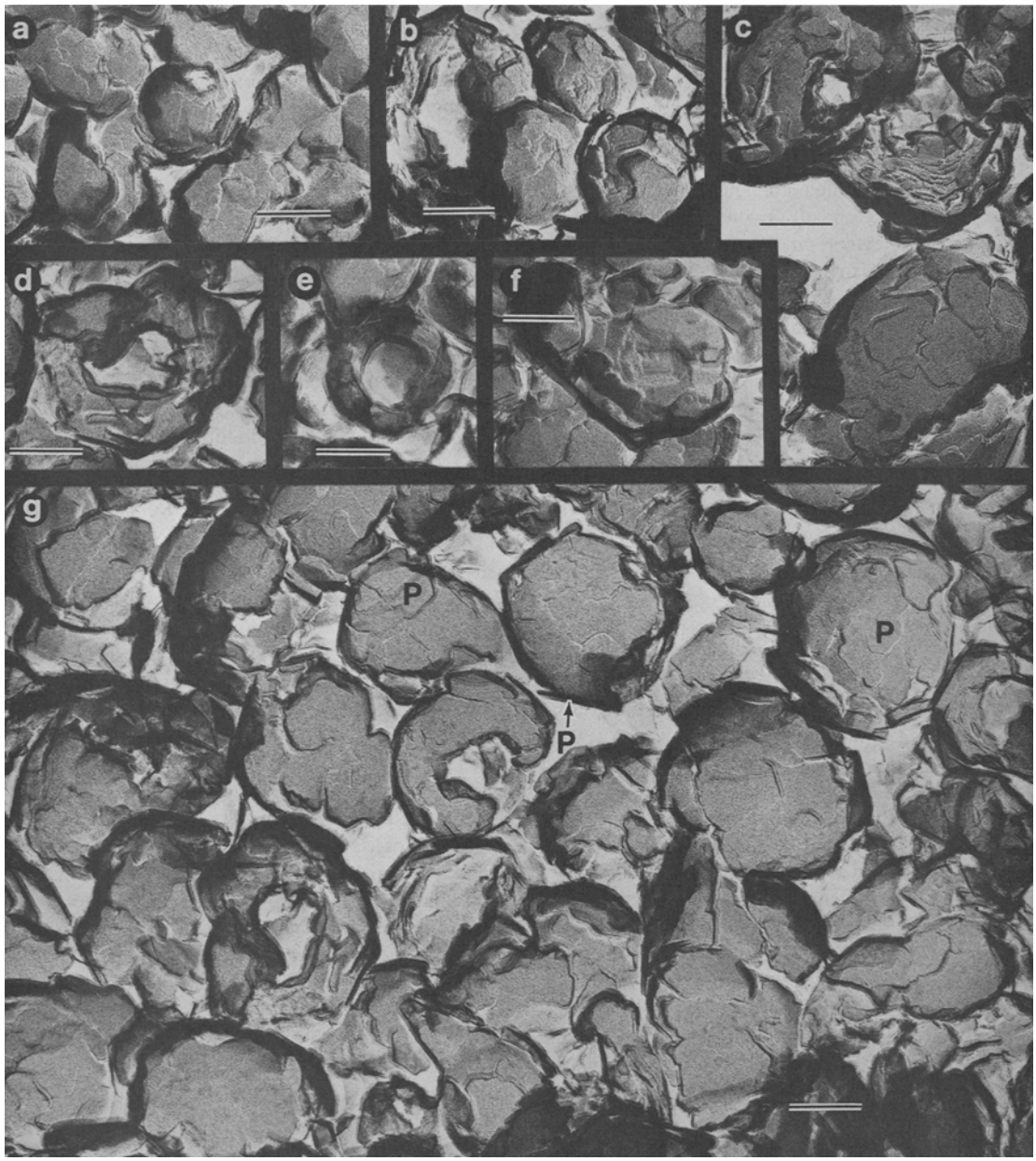

Fig. 6. Transmission electron micrographs of replicas of spheroidal halloysite 2–0·2 μm clay except (a), (e) and (f) which are 0·2–0·08 μm clay.

The poor performance of different methods in the study of halloysite has been a continuing problem, as illustrated by the influence of particle geometry on X-ray intensities. The very high voltages employed in this study show promise for studying interior morphology of larger (0·5 μm dia.) halloysite particles. The replica technique was the most effective method of showing surface morphology. Thin sectioning of spheroids is more difficult than for tubes. The tubular halloysite has more surface exposed for bonding of the cement and the tubes reported had smaller average diameter than the spheres. The spheres generally had a larger hollow cavity than the tubes. Only when the spheroidal cavity was filled with embedding medium was complete embedding obtained (Figs. 7a and c).

The presence of open space between sections of

https://doi.org/10.1346/CCMN.1974.0220118 Published online by Cambridge University Press

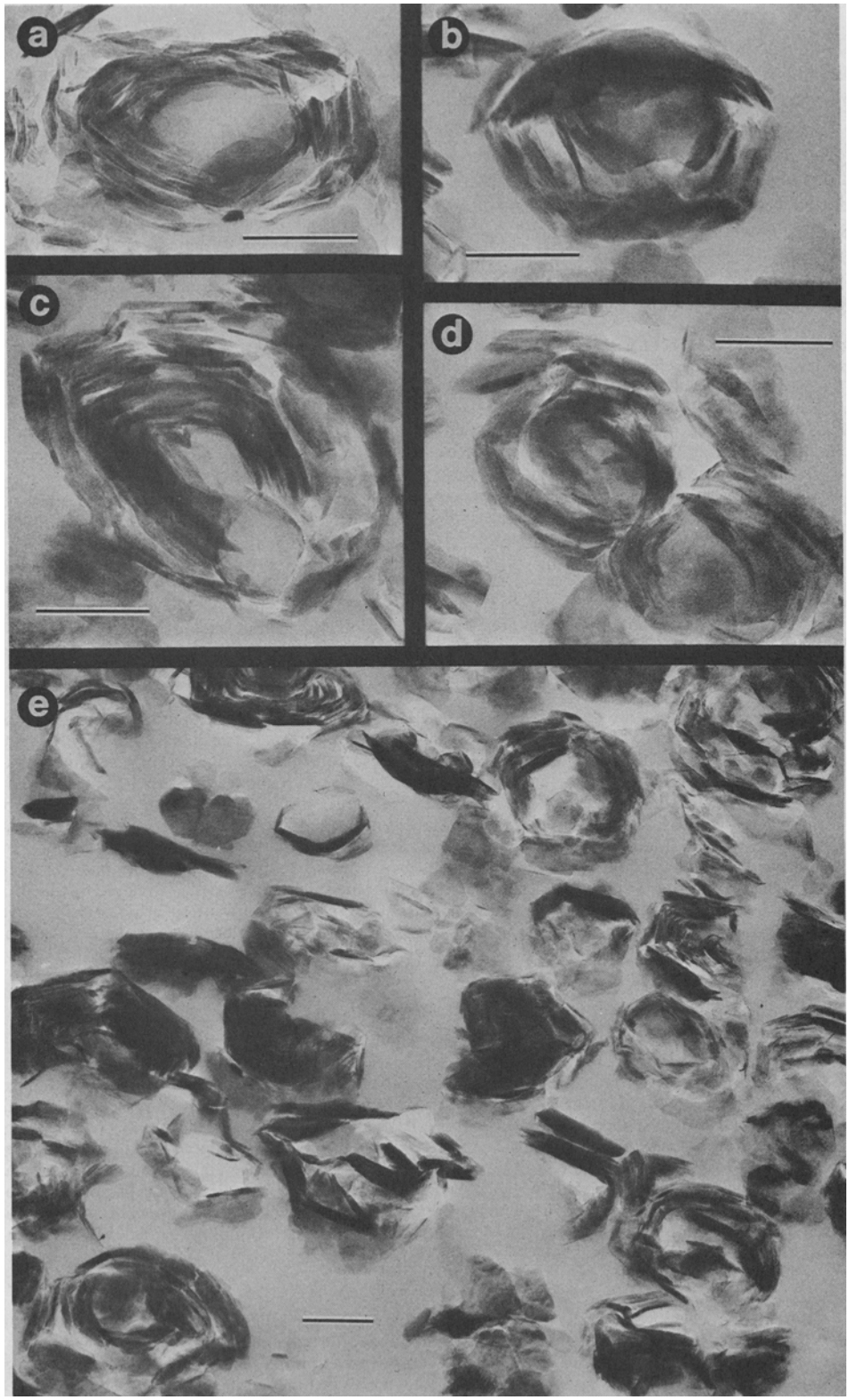

Fig. 7. Transmission electron micrographs of thin sections of spheroidal halloysite 2–0·2 μm clay.

https://doi.org/10.1346/CCMN.1974.0220118 Published online by Cambridge University Press

tubular halloysite polyhedra (Figs. 4e and f) resembles replicas of halloysite tubes studied by Chukhrov and Zvyagin (1966). Interlayer separation parallel to the *a–b* plane between packets of layers is an additional interior feature revealed by direct viewing of thin tubes, thin sections of tubes and high voltage micrographs of spheroids. Each of these forms of interlayer space in dehydrated halloysite probably can be correlated with packing of layers in tubes or spheroids, interior surface area, dehydration rate, solubility rate and diffraction intensity of halloysite particles.

Acknowledgements—The authors wish to thank Dr. E. L. Thurston for use of facilities in the Electron Microscopy Center at Texas A & M University during this study. We also express appreciation to Dr. U. G. Whitehouse, J. R. Scott and J. L. Brown for helpful discussions on the microscopy techniques employed. We gratefully acknowledge the services of D. F. Harling, JEOL (U.S.A.), Inc. Medford, Massachusetts in preparation of the 200 kV micrographs and of the U.S. Steel Corp. Research Center, Monroeville, Pennsylvania for providing the 800 kV micrographs.

REFERENCES

Askenasy, P. E., Dixon, J. B. and McKee, T. R. (1973) Spheroidal halloysite in a Guatemalan soil: *Soil Sci. Soc. Amer. Proc.* **37,** 799–803.

Bates, T. E. (1971) The kaolin minerals. In *The Electron-Optical Investigations of Clays,* (Edited by Gard, J. A.), pp. 109–157. Mineralogical Society, London.

Brindley, G. W. (1961) Kaolin, serpentine and kindred minerals. In *The X-ray Identification and Crystal Structures of Clay Minerals,* (Edited by Brown, G.), pp. 51–131. Mineralogical Society, London.

Brown, J. L. and Rich, C. I. (1968) High resolution electron microscopy of muscovite: *Science* **161,** 1135–1137.

Chukhrov, F. V. and Zvyagin, B. B. (1966) Halloysite, a crystallochemically and mineralogically distinct species: *Proc. of Int. Clay Conf.,* Jerusalem, Israel, **1,** 11–25.

Dixon, J. B. and McKee, T. R. (In Press) Spheroidal halloysite formation in a volcanic soil of Mexico. *Transactions of the 10th International Congress of Soil Science.* Moscow, U.S.S.R.

Jackson, M. L. (1956) *Soil Chemistry-Advanced Course.* Published by the author. Madison, Wisconsin.

Kittrick, J. A. (1969) Soil minerals in the Al_2O_3–SiO_2–H_2O system and a theory of their formation: *Clays and Clay Minerals* **17,** 157–167.

Parham, W. E. (1969) Formation of halloysite from feldspar: Low temperature, artificial weathering vs natural weathering: *Clays and Clay Minerals* **17,** 13–22.

Parham, W. E. (1970) Clay mineralogy and geology of Minnesota's kaolin clays. *Minn. Geol. Survey* **SP-10,** 26–45.

Yada, K. (1967) Study of chrysotile asbestos by a high resolution electron microscope: *Acta. Cryst.* **23,** 704–707.

Résumé—Une halloysite tubulaire de Wagon Wheel Gap, Colorado, et une halloysite sphéroïdale de Redwood County, Minnesota, ont été examinées par microscopie électronique en transmission. Les échantillons d'argile ont été préparés selon les procédés suivants: suspension déposée en goutte sur films support de carbone; sections fines d'argile dans une résine Araldite époxy; répliques carbone–platine–palladium.

Les deux types d'halloysite deshydratée montrent une séparation entre les paquets de feuillets. Les tubes d'halloysite sont composés de paquets dont l'épaisseur peut être réduite à cinq feuillets; ils révèlent parfois sur les vues en section droite une configuration interne enroulée. Les tubes plus épais sont composés de nombreux feuillets par paquet. En section, certains gros tubes apparaissent comme des paquets repliés de feuillets. La morphologie interne des particules d'halloysite sphéroïdale est plus irrégulière et la structure des feuillets est plus discontinue que dans la plupart des tubes. L'halloysite sphéroïdale de ce travail est caractérisée par la présence de plaquettes externes tangentes dont la forme hexagonale ressemble à la kaolinite.

Kurzreferat—Röhrchenförmiger Halloysit von Wagon Wheel Gap, Colorado, und kugelförmiger Halloysit von Redwood County, Minnesota, wurden mit dem Transmissionselektronenmikroskop untersucht. Die Tonproben wurden nach folgenden Methoden präpariert: Auftropfen der Suspension auf Kohlenstoffilm als Träger, Dünnschnitte von Ton in Araldit-Epoxyharz und Kohlenstoff–Platin–Palladium-Replicas. Beide Arten von dehydratisiertem Halloysit weisen Zwischenschichtaufweitungen zwischen den Schichtpaketen auf. Die Halloysitröhrchen sind aus dünnen Paketen zusammengesetzt, die nur aus fünf Schichten bestehen und manchmal bei Betrachtung des Querschnittes im Innern eine aufgerollte Anordnung zeigen. Dickere Röhrchen sind aus vielen Schichten je Schichtpaket zusammengesetzt. Einige große Röhrchen erscheinen im Querschnitt als gefaltete Schichtpakete. Die innere Morphologie der kugelförmigen Halloysitteilchen ist unregelmäßiger und die Schichtstruktur unstetiger als die der meisten Röhrchen. Der hier untersuchte kugelförmige Halloysit ist durch äußere tangentiale Plättchen mit hexagonaler Form charakterisiert, die auf Kaolinit hindeuten.

Резюме — Просвечивающей электронной микроскопией исследовались трубчатый галлуазит из Вагон Хвил Кап, Колорадо, и галлуазит шаровидной формы из района Редвуд, Миннесота. Образцы для исследования под микроскопом приготовили тремя способами: разбавленные водные суспензии образцов глины капали на угольные пленки; тонкие срезы глины приготовили в эпоксидной смоле методом Аралдит; одноэтапную реплику приготовили экранированием платиной-палладием и разбрызгиванием на тонком слое угля.

Оба типа дегидратированных галлуазитов отличаются разобщением пласта между слоями. Трубы галлуазита образуются из настолько тонких пластов, что в них только 5 слоев, которые иногда в разрезе выглядят свернутыми. Пласты толстых труб состоят из многих слоев. Некоторые крупные трубы в разрезе представляют собой свернутые слои. Внутренняя морфология частиц шаровидных галлуазитов более беспорядочная и структура слоев более перерывистая, чем в большинстве труб. В этом анализе шаровидный галлуазит характеризуется внешними тангенциальными шестиугольными пластинками, напоминающими каолинит.

Галлуазит встречается различных морфологических форм (Бэтс, 1971). Трубчатый и шарообразный галлуазиты географически широко распространены в почвах и выветрелых горных породах (Ашкенази, Диксон и МкКее, 1973; Парам, 1969). Расположение каолинитовых слоев в этих частицах различных форм представляет большой интерес. Чухров и Звягин (1966) обратили внимание на многогранные трубы галлуазита, соостоящих из радиальных зон с пластами расположенными параллельно к оси трубы, между радиальными зонами заметили пустоты. Целью настоящего исследования является определение тонких морфологических характеристик двух важных типов галлуазита посредством нескольких методов электронной микроскопии.

https://doi.org/10.1346/CCMN.1974.0220118 Published online by Cambridge University Press